NCCN and NCCCCN Formation in Titan's Atmosphere: 2. HNC as a Viable Precursor

Simon Petrie*,† and Yoshihiro Osamura‡

Department of Chemistry, the Faculties, Australian National University, Canberra ACT 0200 Australia, and Department of Chemistry, Rikkyo University, 3-34-1 Nishi-ikebukuro Tokyo 171-8501, Japan

Received: December 11, 2003; In Final Form: February 8, 2004

Quantum chemical calculations, at the CCSD(T)/aug-cc-pV*X*Z//B3-LYP/6-311G** (X = D, T) levels of theory, have been used to characterize stationary points on the C_2HN_2 and C_4HN_2 potential energy surfaces. The calculations permit evaluation of the reactions of CN ($X\ ^2\Sigma^+$) and C_3N ($X\ ^2\Sigma^+$) with the isomers HNC and HCN, which have been proposed as possible sources of the dicyanopolyynes NCCN and NCCCCN within Titan's upper atmosphere. In keeping with previous studies, we find that the reaction of CN ($X\ ^2\Sigma^+$) with HCN is inhibited by a significant activation energy barrier for all feasible product channels, while CN ($X\ ^2\Sigma^+$) + HNC lacks an overall barrier to formation of NCCN + H (^{2}S) and to HCN + CN ($X\ ^2\Sigma^+$) with the NCCN product channel likely dominant. The C_4HN_2 surface, studied here for the first time, does not possess overall barriers for the processes C_3N ($X\ ^2\Sigma^+$) + HNC → NCCCCN + H (^{2}S), C_3N ($X\ ^2\Sigma^+$) + HNC → C_3N ($X\ ^2\Sigma^+$) + HCN, C_3N ($X\ ^2\Sigma^+$) + HCN → NCCCCN + H (^{2}S), and HC_3N + CN ($X\ ^2\Sigma^+$) → NCCCCN + H (^{2}S). We discuss the implications of these results, and the implied high efficiency of dicyanopolyyne formation in the reactions found to lack overall barriers, for the upper atmospheric chemistry of Titan.

Introduction

Dicyanogen, NCCN, is one of the most distinctive larger molecules to have been identified as a trace constituent within the upper atmosphere of the large Saturnian moon Titan.[1,2] More recently, a larger homologue NCCCCN has also been detected within this object.[3,4] The observation of these compounds, which are the two smallest members of the dicyanopolyyne series, has engendered speculation on the methods by which they are produced under the low-temperature conditions ($T \sim 200$ K) that hold sway in Titan's atmosphere. Following the Voyager encounters with Titan in 1980, the first detailed model of Titanian atmospheric photochemistry[5] incorporated NCCN formation by the reaction

$$\mathrm{HCN} + \mathrm{CN}\ (X\ ^2\Sigma^+) \rightarrow \mathrm{NCCN} + \mathrm{H}\ (^2\mathrm{S}) \qquad (1)$$

with an ascribed rate coefficient of 3.1×10^{-11} cm^3 molecule^{-1} s^{-1}. However, experimental studies[6−9] of reaction 1 have revealed that this process is inhibited by an activation energy barrier. At 200 K, the extrapolated rate coefficient expected is $\sim 5 \times 10^{-15}$ cm^3 molecule^{-1} s^{-1},[8,9] much too low to account for the observed NCCN in Titan's atmosphere. A subsequent revision to the chemical model[10] proposed a reaction sequence

$$\mathrm{N}\ (^2\mathrm{D}) + \mathrm{C_2H_2} \rightarrow \mathrm{HCCN}\ (^3\mathrm{A''}) + \mathrm{H}\ (^2\mathrm{S}) \qquad (2)$$

$$\mathrm{HCCN}\ (^3\mathrm{A''}) + \mathrm{N}\ (^4\mathrm{S}) \rightarrow \mathrm{NCCN} + \mathrm{H}\ (^2\mathrm{S}) \qquad (3)$$

for C_2N_2 formation, and the process

$$\mathrm{HCCN}\ (^3\mathrm{A''}) + \mathrm{HCCN}\ (^3\mathrm{A''}) \rightarrow \mathrm{NCCCCN} + \mathrm{H_2} \qquad (4)$$

for production of the then newly observed NCCCCN molecule.[3] The reaction set 2−4, of which only the initial process 2 has received significant attention via experimental or theoretical study[11−14], has continued to be used in recent models of Titan's atmospheric chemistry (see, for example, the models of Toublanc et al.[15] and Lara et al.[16]) as the principal path to dicyanopolyyne generation. However, as noted in the preceding paper,[17] the "cyanomethylene route" now appears to be very dramatically less effective in producing Titanian NCCN and NCCCCN than was previously thought.

One further possible route to NCCN has recently been identified:[18]

$$\mathrm{HNC} + \mathrm{CN}\ (X\ ^2\Sigma^+) \rightarrow \mathrm{NCCN} + \mathrm{H}\ (^2\mathrm{S}) \qquad (5)$$

and an analogous process

$$\mathrm{HNC} + \mathrm{C_3N}\ (X\ ^2\Sigma^+) \rightarrow \mathrm{NCCCCN} + \mathrm{H}\ (^2\mathrm{S}) \qquad (6)$$

can be envisaged for NCCCCN production. While hydrogen isocyanide (HNC) has not yet been detected within Titan's atmosphere,[19] numerous studies[20−24] have identified HNC as a major product of dissociative recombination of $HCNH^+$, the most abundant ion in Titan's ionosphere.[25−29] In recent work,[18] we have used the CBS−RAD computational procedure, an ab initio technique specifically developed to characterize open-shell species to high accuracy[30], to show that reaction 5 lacks an activation barrier and is therefore apparently feasible as a low-temperature pathway to NCCN. The efficiency of the reaction of CN ($X\ ^2\Sigma^+$) with HNC takes on additional significance as a potential Titanian process since it transpires that most other radicals encountered at high altitudes (e.g., H (^{2}S), CH_3 (^{2}A′), N (^{4}S)) are *not* markedly reactive with HNC.[31]

The preceding paper[17] has explored competing reactions which effectively act to minimize formation of dicyanopolyynes via the cyanomethylene route represented by reactions 2−4. In this work, we present a detailed analysis of the C_2HN_2 potential energy surface, including an exploration of several possible

* Corresponding author. E-mail: simon.petrie@anu.edu.au.
† Australian National University.
‡ Rikkyo University.

10.1021/jp0378182 CCC: $27.50
Published on Web 03/20/2004

TABLE 1: Total and Relative Energies for Stationary Points on the C_2HN_2 Potential Energy Surface at the CCSD(T)/aug-cc-pVTZ//B3-LYP/6-311G Level of Theory**

		CCSD(T)/aug-cc-pVTZ//B3-LYP/6-311G**				CBS−RAD
species	label	E_e[a] Hartree	ZPE[b] mHartree	E_0[c] Hartree	E_{rel}[d] kJ mol^{-1}	E_{rel}[d,e] kJ mol^{-1}
HNC + CN ($X\ ^2\Sigma^+$)	r_5	−185.829868	20.618	−185.809250	0.0	0.0
HNC•CN[f]	$int_5$1[f]	−185.835233	20.940	−185.814293	−13.2	−9.2
HNC···CN[f]	TS_5 1−2[f]	−185.837037	20.680	−185.816357	−18.7	−18.0
HNCCN	$int_5$2	−185.912067	25.627	−185.886440	−202.7	−211.7
H···NCCN	TS_5 2-A	−185.854916	17.059	−185.837857	−75.1	−84.8
NCCN + H (^{2}S)	p_5A	−185.864406	16.543	−185.847863	−101.4	−108.9
N(H)CCN	TS_5 2−3	−185.843577	20.286	−185.823291	−36.9	−40.2
NCHCN	$int_5$3	−185.917315	25.573	−185.891742	−216.6	−219.1
NC(···H)CN	TS_5 3-A	−185.854144	17.486	-185.836658	−72.0	−79.9
NC(H)···CN	TS_5 3-B	−185.851228	21.799	-185.829429	−52.9	−53.4
HCN + CN ($X\ ^2\Sigma^+$)	p_5B	−185.853350	21.424	−185.831926	−59.5	−56.1
CN(H)···CN	TS_5 r-4	−185.813972	21.950	−185.792022	45.2	48.0
CNHCN	$int_5$4	−185.847546	25.792	−185.821754	−32.8	−30.0
CN(···H)CN	TS_5 4-C	−185.799253	17.357	−185.781896	71.8	72.4
CNCN + H (^{2}S)	p_5C	−185.825287	15.829	−185.809458	−0.5	−8.5
C(H)NCN	TS_5 4−7	−185.785698	19.204	−185.766494	112.3	
HCNCN	$int_5$7	−185.892407	25.349	−185.867059	−151.8	
HCN···CN	TS_5 7-B	−185.846618	21.637	−185.824981	−41.3	
H···CNCN	TS_5 7-C	−185.823873	16.103	−185.807771	3.9	
HNC···NC	TS_5 r-8	−185.822378	20.827	−185.801551	20.2	
HNC(CN)	TS_5 2−8	−185.841277	23.224	−185.818053	−23.1	
HNCNC	$int_5$8	−185.880716	25.504	−185.855212	−120.7	
H···NCNC	TS_5 8-C	−185.814647	16.339	−185.798308	28.7	
N(H)CNC	TS_5 8−5	−185.811543	19.402	−185.792141	44.9	
NC(H)NC	$int_5$5	−185.884254	25.102	−185.859152	−131.0	−131.7
NC(H)···NC	TS_5 5-B	−185.833851	21.723	−185.812128	−7.6	−6.0
NC(···H)NC	TS_5 5-C	−185.814910	16.917	−185.797993	29.6	28.7
NC···HNC	TS_5 r-6	−185.809149	16.903	−185.792246	44.6	46.2
NCH•NC	$int_5$6	−185.858029	22.358	−185.835671	−69.4	−66.5

[a] Total energy, excluding ZPE. [b] Corrected zero-point energy, according to B3-LYP/6-311G** calculations. [c] Total energy (at zero Kelvin) including ZPE. [d] Energy relative to the reactants CN + HNC, at zero K. [e] From ref 18. [f] This stationary point was not found at the B3-LYP/6-311G** level of theory. The QCISD/6-31G* optimized geometry (ref 18) was employed instead.

product channels not encompassed in an earlier study of this surface.[18] We investigate also, for the first time, the C_4HN_2 potential energy surface relevant to occurrence of reaction 6. The reliability of the quantum chemical techniques employed here is particularly important in the context of HNC reaction chemistry, since the transient nature of hydrogen isocyanide under laboratory conditions effectively obstructs experminental study of its reactions with other neutrals.

Theoretical Methods

The hybrid density functional method combining Becke's three-parameter exchange functional[32] with the correlation functional of Lee, Yang, and Parr[33] (B3-LYP) was used, with the triple-split-valence 6-311G** Gaussian basis set,[34] in geometry optimizations and vibrational frequency calculations for all stationary points sought on the C_2HN_2 and C_4HN_2 potential energy surfaces. These calculations were executed using the GAUSSIAN98 program suite,[35] while the MOLPRO2002 quantum chemical package[36] was applied for the subsequent coupled-cluster with single, double, and perturbative triple excitations (CCSD(T)) single-point calculations featuring the augmented correlation-consistent basis sets of Dunning and co-workers.[37] The augmented triple-ζ (aug-cc-pVTZ) basis set was used in calculations on the C_2HN_2 stationary points, while the smaller, analogous augmented double-ζ (aug-cc-pVDZ) basis set was used for the C_4HN_2 stationary points.

The combination of B3-LYP optimized geometries and CCSD(T) single-point total energies has been widely used in several previous studies on radical-neutral reactions, in many instances providing opportunities for direct comparison with experimental kinetic and dynamic results.[38−40] These comparisons have established the general reliability of this computational approach, strengthening confidence in the validity of the present calculations concerned, at least in part with reactions of HNC for which no comparison with experimental data is currently possible.

Results and Discussion

1. The C_2HN_2 Potential Energy Surface. The stationary points characterized on the C_2HN_2 potential energy surface (PES), at the CCSD(T)/aug-cc-pVTZ//B3-LYP/6-311G** level of theory, are summarized in Table 1, which details their calculated total energy as well as their energy relative to that of the reactant pair HNC + CN ($X\ ^2\Sigma^+$). A comment here is pertinent to highlight the notation that we have employed to distinguish C_2HN_2 stationary points (identified by a subscript '5') from their analogues on the C_4HN_2 surface (bearing a '6' subscript), which are also discussed in this work. The subscripts indicate the relevance of a stationary point to either reaction 5 or reaction 6, while the use of 'r', 'p', 'int', and 'TS' labels denotes respectively the identity of the various species as reactants, products, intermediates, or transition states.

For purposes of comparison, in Table 1 we have furnished also the CBS−RAD relative energies for several of these stationary points, as obtained in an earlier study of the C_2HN_2 surface.[18] The portion of the PES that was not examined in the earlier study[18] principally concerns stationary points relevant to CNCN formation, and optimized geometries for these "new" stationary points are provided in Figure 1.

The agreement between the CCSD(T)/aug-cc-pVTZ (this work) and CBS−RAD[18] relative energies, in Table 1, is good.

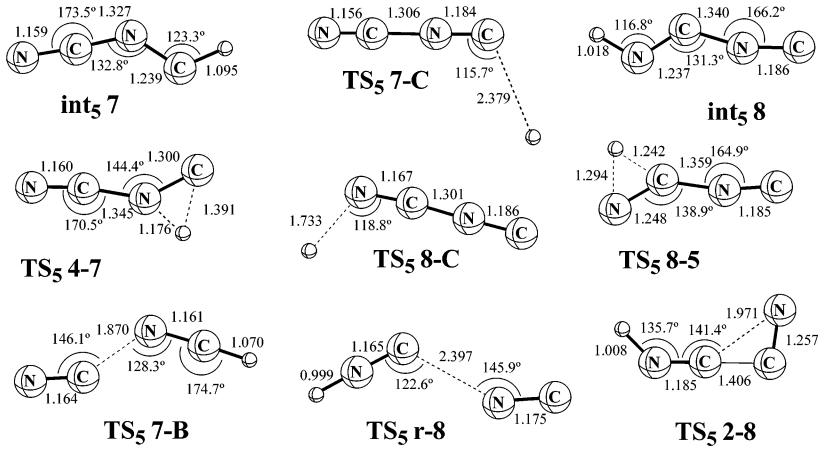

Figure 1. Geometries of some stationary points obtained on the C_2HN_2 potential energy surface, at the B3-LYP/6-311G** level of theory. Bond lengths are shown in Å, while bond angles (in degrees) are only shown when they do not exceed 175°. The stationary points shown are restricted to those for which optimized geometries have not been reported previously (ref 18).

The largest discrepancy between the two methods is the 9.7 kJ mol^{-1} difference in relative energies found for the transition structure TS_5 2-A, corresponding to the H-loss channel from the reactive intermediate HNCCN ($int_5$2). Despite the different approaches used for geometry optimization in the two levels of theory (CBS−RAD uses geometries optimized at the QCISD/6-31G* level of theory), all portions of the surface common to both studies show very similar features.[41] Most importantly, both CBS−RAD and CCSD(T)/aug-cc-pVTZ calculations indicate that the HNC + CN → HNCCN entrance channel is not impeded by an activation energy barrier, despite the occurrence of such a barrier (TS_5 1−2) on the surface at the QCISD/6-31G* level of theory. This barrier does not feature on the B3-LYP/6-311G** surface, so to substantiate its absence at the CCSD(T)/aug-cc-pVTZ level we have employed the QCISD/6-31G* optimized geometry for this putative stationary point in the present calculations. Both the CBS−RAD[18] and the CCSD(T) calculations using this geometry find a total energy for this structure that is lower than that of an apparent preceding weakly bound minimum (HNC·CN ($int_5$1), also found at the QCISD/6-31G* level but not at B3-LYP/6-311G**), therefore implying that the apparent entrance-channel transition structure TS_5 1−2 is an artifact of the QCISD/6-31G* level of theory. The evaporation of this PES feature when a sufficiently high level of theory is employed is very similar to the phenomenon that we have noted previously for the reactions of C_2H ($X\ ^2\Sigma^+$) with HNC (which possesses an entrance channel barrier at the CISD/DZ+P[42] and QCISD/6-31G* [31] levels of theory, but not at B3-LYP/6-311+G**,[31] CBS−RAD,[31] or CCSD(T)/cc-pVTZ)[42] and CN ($X\ ^2\Sigma^+$) + HCCH (where, again, an entrance channel barrier is obtained in CISD/DZ+P geometry optimizations but is not substantiated in CCSD(T)/cc-pVTZ single-point calculations).[42]

Interpretation of the C_2HN_2 PES features may be more easily implemented by reference to the schematic diagram given in Figure 2. It is apparent that, starting from reactants HNC + CN, only the addition−elimination processes leading to formation of NCCN + H and to HCN + CN are feasible in the sense of lacking any protruding activation energy barriers. Two viable pathways to NCCN + H have been identified:

$$\mathrm{HNC + CN \rightarrow HNCCN\ (int_5 2) \rightarrow TS_5\ 2\text{-}A \rightarrow NCCN + H}$$

and

$$\mathrm{HNC + CN \rightarrow int_5 2 \rightarrow TS_5\ 2{-}3 \rightarrow NCC(H)N\ (int_5 3) \rightarrow TS_5\ 3\text{-}A \rightarrow NCCN + H}$$

and one to HCN + CN:

$$\mathrm{HNC + CN \rightarrow int_5 2 \rightarrow TS_5\ 2{-}3 \rightarrow int_5 3 \rightarrow TS_5\ 3\text{-}B \rightarrow HCN + CN}$$

with the first of these three processes being clearly the most direct, as well as featuring the most deeply submerged intervening barrier. In contrast, the only viable channel leading to HCN production features significantly higher submerged barriers than do either of the above channels leading to NCCN formation. We therefore envisage that production of NCCN + H will be the most efficient pathway of the HNC + CN reaction at low temperatures.

While a great many other possible reaction pathways can be conjectured, our analysis of the PES indicates that all bimolecular pathways other than the three detailed above are hindered by barriers that protrude above the total energy of reactants HNC + CN by a significant margin. These energetically disfavored pathways include all of the routes explored for formation of CNCN + H, as well as the direct formation of HCN + CN by H-atom abstraction from HNC. Our calculations show a modest barrier (of 6.6 kJ mol^{-1}) to conversion of HCN + CN reactants to NCCN + H, in good agreement with laboratory studies which show this process to be very inefficient at low temperatures.[8,9] It is also evident, from Figure 2, that there is no viable low-temperature route for conversion of reactant CNCN + H to NCCN + H. Note, however, that our calculated barrier for the reaction CNCN + H → HCN + CN (which has not yet received experimental study) is only 4.4 kJ mol^{-1} in height. Therefore, within the expected accuracy of our calculations, we cannot rule out the viability of the latter process at Titanian atmospheric temperatures, although CNCN has not been detected within Titan's atmosphere, nor has any scheme for its formation been developed.

2. The C_4HN_2 Potential Energy Surface: Comparison with the C_2HN_2 Surface. Our CCSD(T)/aug-cc-pVDZ//B3-LYP/6-311G** exploration of the C_4HN_2 PES is detailed in Table 2. To the best of our knowledge, this is the first examination of this PES to have yet been undertaken. Note that the larger size of species on this PES has necessitated the use of a smaller basis set (augmented double-ζ) than that used in our C_2HN_2 analysis, and this limitation is likely to have reduced the

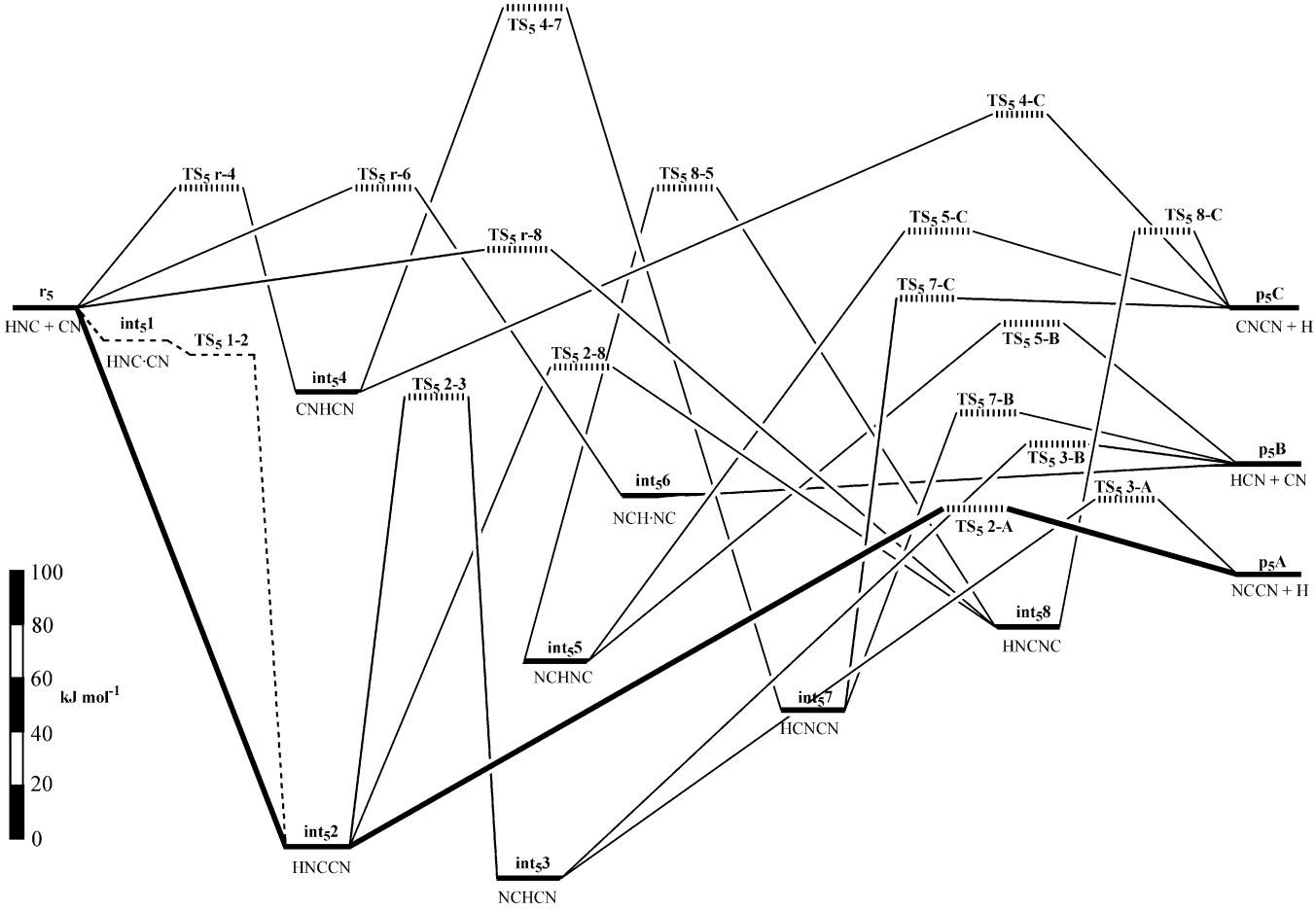

Figure 2. Pathways between stationary points on the C_2HN_2 potential energy surface, characterized at the CCSD(T)/aug-cc-pVTZ//B3-LYP/6-311G** level of theory. The most direct (and most exothermic) reaction pathway, leading to NCCN + H, is shown in bold. The pathway shown as a dotted line features stationary points which exist at the QCISD/6-31G* level of theory, but not at B3-LYP/6-311G**.

accuracy of the relative energies thus obtained for C_4HN_2 stationary points. However, neither the CCSD(T) single-point calculations nor the B3-LYP/6-311G** optimizations identify any of the stationary points as possessing a total energy within ± 10 kJ mol^{-1} of the total energy of reactant C_3N ($X\ ^2\Sigma^+$) + HNC, suggesting that we can comment with reasonable confidence on the presence or absence of any absolute activation energy barriers on product channels for this reaction.

Perusal of the potential energy diagram (Figure 3) for this surface reveals some obvious similarities with the B3-LYP/6-311G** optimized potential energy surface for C_2HN_2. On both surfaces, the radical + HNC entrance channel for C−C bond formation lacks a barrier, and the direct process of H-atom loss from this low-energy intermediate is impeded by a substantially lower barrier than exists for any of the less direct pathways to various products. Of the identified local minima (Figure 4), several also have direct counterparts (with generally very similar geometric features) on the C_2HN_2 PES. The additional local minima, including the cyclic species int$_6$4 and the branched skeletal species int$_6$5 and int$_6$7, represent structural motifs that are not geometrically attainable on the C_2HN_2 surface. However, the increased number of intermediates on the C_4HN_2 surface (compared to C_2HN_2) is not accompanied by a commensurate increase in the number of identifiable transition states (Figure 5). Several of the transition structures that might reasonably be expected for interconversion of the various intermediates, particularly by tautomerization, do not exist on the B3-LYP optimized C_4HN_2 PES. With very few exceptions, it appears that H loss (yielding one or other C_4N_2 isomer) occurs at a lower threshold than H migration. This phenomenon has the curious consequence that, although we can determine barrierless pathways through sequences of intermediate stationary points for all of the reactant pairs C_3N + HNC, C_3N + HCN, and HC_3N + CN leading to NCCCCN + H formation, there is no apparent conventional route leading from reactant C_3N + HNC to the lower-energy possible product HC_3N + CN. We shall enlarge upon this aspect of the PES in the following sections.

3. The C_4HN_2 Potential Energy Surface: Reaction of C_3N ($X\ ^2\Sigma^+$) with HNC. A cursory examination of Figure 3 suggests that the only feasible barrierless processes commencing with reactant C_3N + HNC are

$$C_3N + HNC \rightarrow NCCCCNH\ (int_6 1) \rightarrow TS_6\ 1\text{-A} \rightarrow NCCCCN + H$$

$$C_3N + HNC \rightarrow int_6 1 \rightarrow TS_6\ 1{-}2 \rightarrow NCCCCHN\ (int_6 2) \rightarrow TS_6\ 2\text{-A} \rightarrow NCCCCN + H$$

and

$$C_3N + HNC \rightarrow int_6 1 \rightarrow TS_6\ 1{-}2 \rightarrow int_6 2 \rightarrow C_3N + HCN$$

However, such an analysis supposes that the reaction necessarily proceeds along the minimum energy pathway and terminates at the first opportunity to form products. While it is likely that the product pairs NCCCCN + H (^{2}S) and C_3N ($X\ ^2\Sigma^+$) + HCN do indeed constitute the major product channels of the reaction of C_3N ($X\ ^2\Sigma^+$) with HNC, there is also apparently sufficient

TABLE 2: Total and Relative Energies for Stationary Points on the C_4HN_2 Potential Energy Surface at the CCSD(T)/aug-cc-pVDZ//B3-LYP/6-311G Level of Theory**

species	label	E_e[a] Hartree	ZPE[b] mHartree	E_0[c] Hartree	E_{rel}[d] kJ mol^{-1}
HNC + C_3N ($X\ ^2\Sigma^+$)	r_6	−261.61101	30.13	−261.58089	0.0
NCCCCNH	$int_6$1	−261.71080	34.95	−261.67585	−249.3
NCCCCN···H	TS_6 1-A	−261.65760	27.41	−261.63019	−129.5
NCCCCN + H (^{2}S)	p_6A	−261.66583	26.99	−261.63884	−152.2
NCCCC(H)N	TS_6 1-2	−261.64213	30.22	−261.61190	−81.4
NCCCCHN	$int_6$2	−261.71517	35.89	−261.67927	−258.3
NCCC···C(H)N	TS_6 2-A	−261.65435	27.84	−261.62651	−119.8
HCN + C_3N ($X\ ^2\Sigma^+$)	p_6B	−261.63370	30.86	−261.60284	−57.6
NCCC(···H)CN	TS_6 A-3	−261.65912	27.54	−261.63158	−133.1
NCCCHCN	$int_6$3	−261.74059	36.05	−261.70454	−324.7
HC_3N + CN ($X\ ^2\Sigma^+$)	p_6C	−261.64864	32.12	−261.61652	−93.6
NCCCH(CN)	TS_6 3-4	−261.68582	34.21	−261.65161	−185.7
c-NCC(CN)CH	$int_6$4	−261.68846	35.41	−261.65305	−189.5
c-NCC(···CN)CH	TS_6 4-5	−261.68078	33.78	−261.64699	−173.6
$HCC(CN)_2$	$int_6$5	−261.72982	36.04	−261.69378	−296.4
HCC(···CN)CN	TS_6 5-C	−261.64859	32.33	−261.61626	−92.9
NCCC···HNC	TS_6 r-6	−261.59853	29.67	−261.56885	31.6
NCCCH·NC	$int_6$6	−261.65364	32.86	−261.62078	−104.7
HCCC(···CN)N	TS_6 C-7	−261.64303	32.33	−261.61070	−78.3
HCCC(N)CN	$int_6$7	−261.70595	35.65	−261.67030	−234.8
HCC···C(N)CN	TS_6 7-D	−261.62216	31.15	−261.59101	−26.6
NCCN + C_2H ($X\ ^2\Sigma^+$)	p_6D	−261.62420	30.66	−261.59354	−33.2
NCCC···NHC	TS_6 r-8	−261.60772	31.91	−261.57582	13.3
NCCCNHC	$int_6$8	−261.64635	36.16	−261.61020	−77.0
NCCCN(···H)C	TS_6 8-E	−261.59908	27.74	−261.57134	25.1
NCCCNC + H (^{2}S)	p_6E	−261.62667	26.15	−261.60052	−51.6
NCCCNCH	$int_6$9	−261.68745	34.95	−261.65250	−188.0
CNCCCN···H	TS_6 10-E	−261.61790	26.57	−261.59132	−27.4
CNCCCNH	$int_6$10	−261.66877	33.92	−261.63485	−141.7

[a] Total energy, excluding ZPE. [b] Corrected zero-point energy, according to B3-LYP/6-311G** calculations. [c] Total energy (at zero Kelvin) including ZPE. [d] Energy relative to the reactants C_3N + HNC, at zero K.

internal energy to permit the isomerization process

$$NCCCCHN\ (int_6 2) \leftrightarrow NCCCHCN\ (int_6 3)$$

even though such a process does not possess a recognizable transition structure in the face of competition from H loss. We have confirmed, by a potential energy scan, that retention of the H atom during $int_6$2 ↔ $int_6$3 isomerization can proceed across a region of the PES, which is always submerged by at least 80 kJ mol^{-1} below the total energy of reactants C_3N + HNC at the CCSD(T)/aug-cc-pVDZ//B3-LYP/6-311G** level of theory, and so the production of HC_3N + CN from C_3N + HNC, via the overall pathway

$$C_3N + HNC \rightarrow int_6 1 \rightarrow TS_6\ 1\text{-}2 \rightarrow int_6 2 \rightarrow \rightarrow int_6 3 \rightarrow HC_3N + CN$$

must be regarded as being at least mechanistically feasible.

Similar arguments might be offered for the pathway

$$C_3N + HNC \rightarrow int_6 1 \rightarrow TS_6\ 1\text{-}2 \rightarrow int_6 2 \rightarrow \rightarrow NCCCNCH\ (int_6 9) \rightarrow NCCCNC + H$$

although here the formation of NCCCNC + H requires a skeletal rearrangement from NCCCCHN which is likely to be quite inefficient in competition with direct dissociation to form p_6B, a channel which in any event is slightly more exothermic according to our calculations. Nevertheless, this 'fully submerged' pathway is evidently more accessible at low temperature than the competing process

$$C_3N + HNC \rightarrow TS_6\ r\text{-}8 \rightarrow NCCCNHC\ (int_6 8) \rightarrow TS_6\ 8\text{-}E \rightarrow NCCCNC + H$$

which suffers from protruding activation energy barriers on both the entrance and exit channels.

The final exothermic product combination, NCCN + C_2H, can in principle arise from the pathway

$$C_3N + HNC \rightarrow int_6 1 \rightarrow TS_6\ 1\text{-}2 \rightarrow int_6 2 \rightarrow \rightarrow int_6 3 \rightarrow \rightarrow TS_6\ C\text{-}7 \rightarrow int_6 7 \rightarrow TS_6\ 7\text{-}D \rightarrow NCCN + C_2H$$

However, this convoluted route involves the avoidance of two intervening product formation opportunities (NCCCCN + H from $int_6$2, and HC_3N + CN from $int_6$3), both of which are substantially more exothermic than the NCCN + C_2H product combination. We expect that production of NCCN + C_2H from reactant C_3N + HNC is therefore negligible.

To summarize the PES from the perspective of reactant C_3N ($X\ ^2\Sigma^+$) + HNC, it seems likely that NCCCCN + H (^{2}S) is a major product channel, and may well dominate, although a straightforward route to the less exothermic products C_3N ($X\ ^2\Sigma^+$) + HCN is also available. Production of HC_3N + CN ($X\ ^2\Sigma^+$) is also feasible, though not (at low temperatures) by direct H-atom abstraction, and if NCCCCN formation is the major channel, then HC_3N + CN may (by virtue of its greater exothermicity) compete effectively with the C_3N + HCN channel. Other product combinations (NCCCNC + H, NCCN + C_2H) appear to be substantially disfavored in comparison and likely do not contribute significantly.

4. The C_4HN_2 Potential Energy Surface: Other Reactions. The C_4HN_2 PES also offers very useful insights into the low-temperature reactivity of other combinations of reactants found in significant concentration within Titan's upper atmosphere. First, our calculations establish that although several exothermic product combinations (NCCCCN + H, C_3N + HCN, HC_3N + CN, and NCCCNC + H) exist for internally cold NCCN +

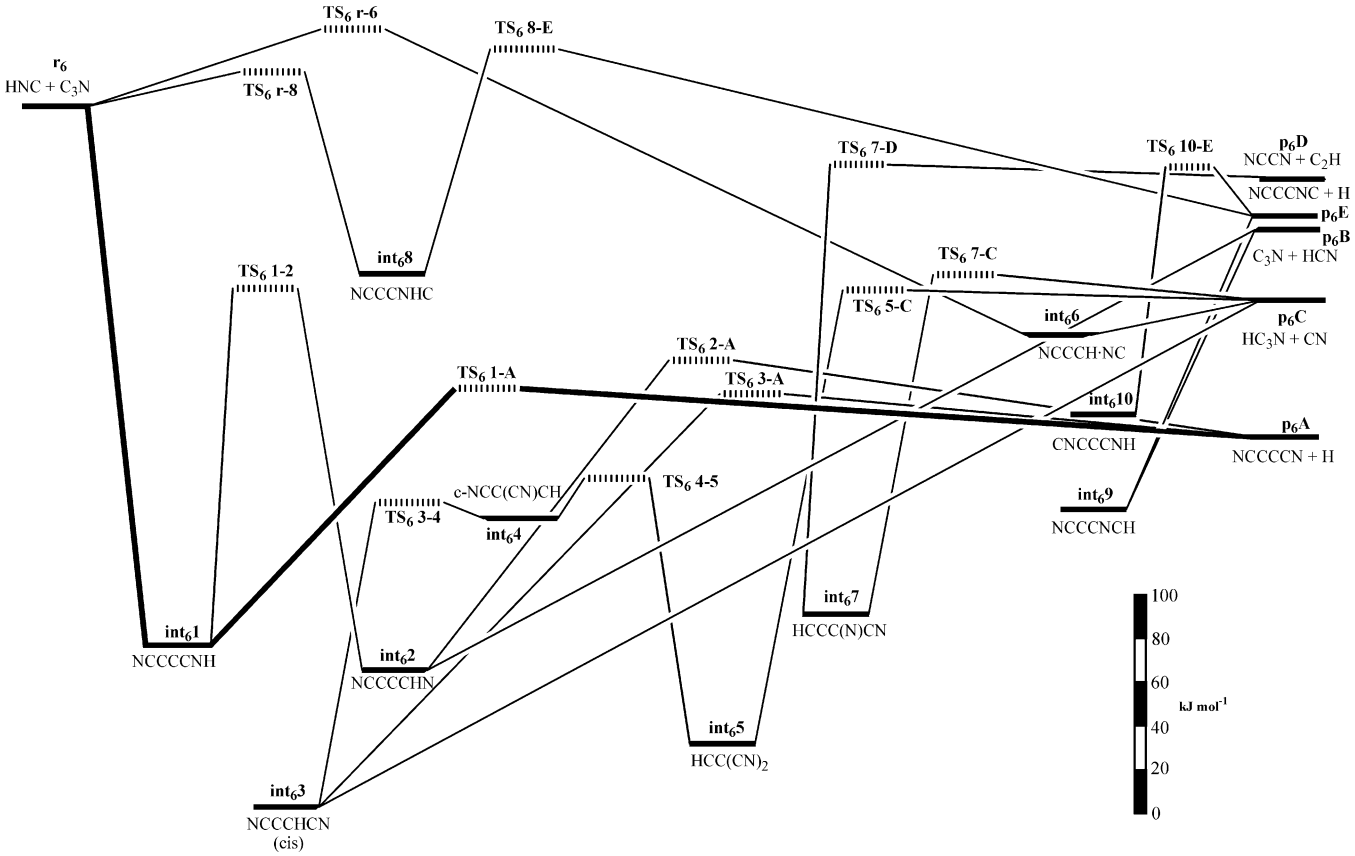

Figure 3. Pathways between stationary points on the C_4HN_2 potential energy surface, characterized at the CCSD(T)/aug-cc-pVDZ//B3-LYP/6-311G** level of theory. The most direct (and most exothermic) reaction pathway, leading to NCCCCN + H, is shown in bold.

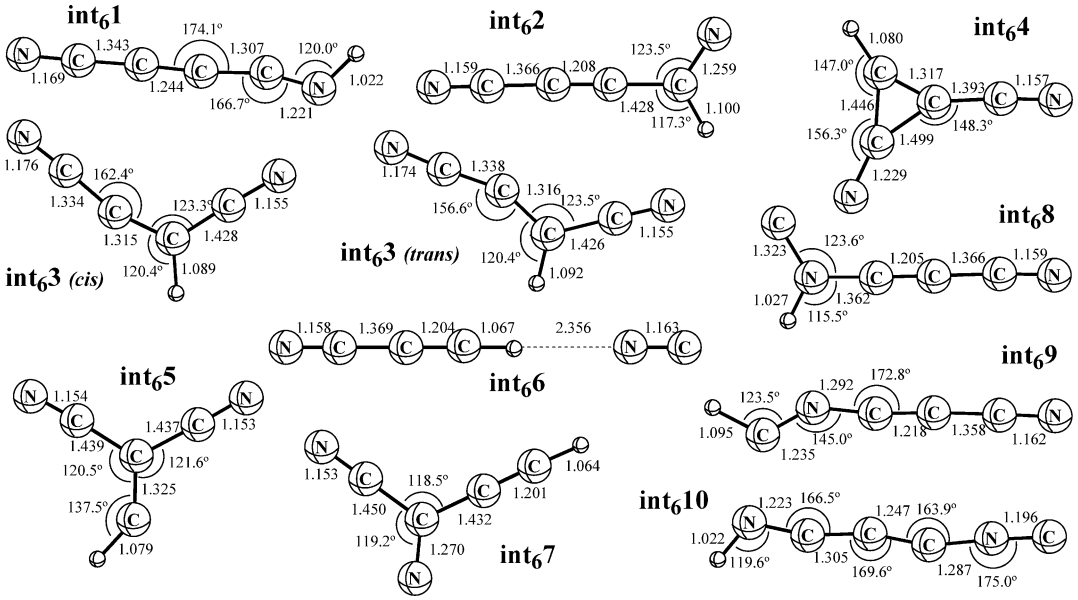

Figure 4. Geometries of local minima obtained on the C_4HN_2 potential energy surface, at the B3-LYP/6-311G** level of theory. Bond lengths are shown in Å, while bond angles (in degrees) are only shown when they do not exceed 175°.

C_2H ($X\ ^2\Sigma^+$) reactants, none of these products appear accessible because of the 6.6 kJ mol^{-1} entrance channel barrier (TS_6 7-D). This slight barrier height, for which experimental verification would be valuable, implies a limiting efficiency of only around 2% of collisions at 200 K for the process

$$NCCN + C_2H \rightarrow TS_6\ 7\text{-}D \rightarrow int_6 7 \rightarrow TS_6\ C\text{-}7 \rightarrow HCCCN + CN$$

Formation of either NCCCCN + H or C_3N + HCN in this system apparently requires passage along the same channel followed by a barrierless transition to $int_6$3 and subsequent traversal of additional regions of the PES shown in Figure 3.

For reactant NCCCNC + H (^{2}S), formation of C_3N + HCN may be essentially quantitative since this process involves only the intermediate $int_6$9 with no intervening transition states on either the entrance or exit channels. NCCCCN + H production is, however, a more exothermic subsequent process (see below) which may compete.

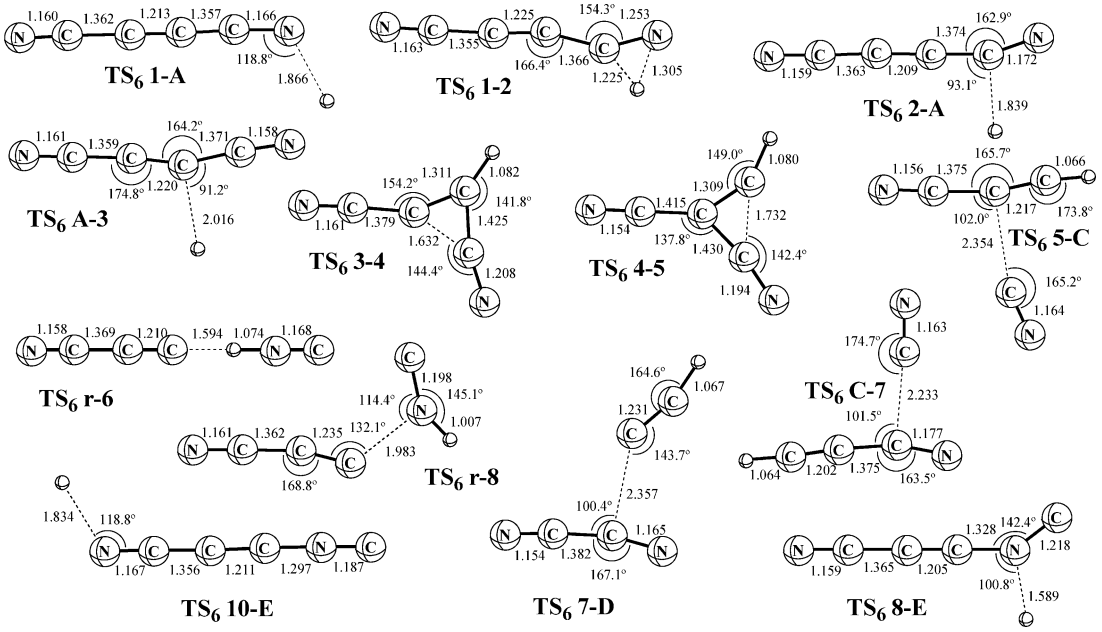

Figure 5. Geometries of transition states obtained on the C_4HN_2 potential energy surface, at the B3-LYP/6-311G** level of theory. Bond lengths are shown in Å, while bond angles (in degrees) are only shown when they do not exceed 175°.

TABLE 3: Loss Processes for HNC within Titan's Upper Atmosphere

		[X]/10^3 molecule cm^{-3} [a]					%loss[d]		
intermediate	reactant X	z = 800	1000	1200	k_{200}[b]	products[c]	z = 800	1000	1200
HNC	CN (X $^2\Sigma^+$)	0.5	1	2.7	3.0×10^{-11} [e]	NCCN + H (^{2}S)	2.4	29	93
	C_3N (X $^2\Sigma^+$)	1.5	0.4	0.005	3.0×10^{-11} [e]	NCCCCN + H (^{2}S)	7	12	0.2
	H (^{2}S)	7.5E(4)	8000	800	7.5×10^{-15} [f]	HCN + H (^{2}S)	90	59	7
	CH_3 (^{2}A′)	6.5E(4)	2E(4)	4000	9.2×10^{-20} [f]	CH_3CN + H (^{2}S)	0.001	0.002	< 0.001

[a] Reactant concentrations in molecule cm^{-3}, at altitudes of 800, 1000, and 1200 km, were obtained by graphical interpolation of data presented in the modeling studies of Banaszkiewicz et al. (ref 29: H, CH_3), Yung (ref 10: CN), and Toublanc et al. (ref 15: CCCN). [b] Rate coefficients in cm^3 molecule^{-1} s^{-1}, at T = 200 K. [c] Expected major product channel of the indicated combination of reactants. [d] Efficiency of the indicated HNC removal mechanism, expressed as a percentage of the total removal rate due to the processes listed here, at the indicated altitude. [e] Ascribed rate coefficient for an exothermic radical/unsaturated neutral reaction lacking an activation barrier. [f] Rate coefficient ascribed according to the Arrhenius expression, with preexponential factor $A = 3.0 \times 10^{-11}$ cm^3 molecule^{-1} s^{-1} and activation energy E_a as obtained in a recent CBS−RAD study of the relevant potential energy surface (ref 31).

The reaction of C_3N (X $^2\Sigma^+$) + HCN is likely to result principally in NCCCCN + H products, since this is both the more direct

$$C_3N + HCN \rightarrow int_6 2 \rightarrow TS_6\ 2\text{-A} \rightarrow NCCCCN + H$$

and the more exothermic channel in competition with HC_3N + CN

$$C_3N + HCN \rightarrow int_6 2 \rightarrow TS_6\ 2\text{-A} \rightarrow \rightarrow TS_6\ 3\text{-A} \rightarrow int_6 3 \rightarrow HC_3N + CN$$

Finally, HC_3N + CN (X $^2\Sigma^+$) can apparently give rise only to NCCCCN + H, a process expected to be highly efficient by virtue of the absence of an entrance channel barrier. The most elevated stationary point within the sequence

$$HC_3N + CN \rightarrow int_6 3 \rightarrow TS_6\ 3\text{-A} \rightarrow NCCCCN + H$$

has a relative energy (cf. reactant HC_3N + CN) of −75.5 kJ mol^{-1}. The reaction of HC_3N + CN has been studied using flash photolysis, with a measured rate coefficient of 1.69×10^{-11} cm^3 molecule^{-1} s^{-1} at 298 K.[43] The much greater rate coefficient for this reaction, than for the analogous reaction of HCN + CN (for which recent studies have indicated a 298 K rate coefficient of 3.2×10^{-14} cm^3 molecule^{-1} s^{-1}),[8,9] is in agreement with our determination of an activation energy barrier to the HCN reaction, but not to the reaction involving HC_3N.

5. Implications of These Results for Formation of Titanian NCCN and NCCCCN. A detailed and quantitative assessment of these processes, in the context of Titanian atmospheric chemical evolution, must await their inclusion within rigorous chemical modeling networks such as the coupled ion/neutral model of Banaszkiewicz et al.[29] For the present, we base our assessment largely on a comparison of the loss processes for the key intermediates HCCN (^{3}A″) (as featured in the preceding paper)[17] and HNC (see Table 3). For HNC loss, we consider again the same altitude range of 800 to 1200 km identified as most effective for NCCN production by the cyanomethylene route.[10,15]

In contrast to our comparison of triplet HCCN loss processes,[17] the data within Table 3 suggest that dicyanopolyyne formation is an important loss process for Titanian HNC, with NCCN production apparently the dominant fate of HNC at an altitude of 1200 km. The importance of the reactions of CN and, to a lesser extent, of CCCN, with HNC derives largely from the expected high efficiency of these processes, in contrast to the very much lower efficiency ascribed to the barrier-inhibited[31] reactions of the much more abundant H and CH_3 radicals.

TABLE 4: Estimation of Formation Rates for NCCN and NCCCCN within Titan's Upper Atmosphere

	[X]/10^3 molecule cm^{-3} [a]				[Y]/10^3 molecule cm^{-3} [a]				formation rate/10^{-5} cm^{-3} s^{-1} [c]		
reactant X	z = 800	1000	1200	reactant Y	z = 800	1000	1200	k_{200}[b]	z = 800	1000	1200
HCCN (^{3}A″)	0.25	2	0.2)	N (^{4}S)	1.3	8	10	1.0×10^{-12} [d]	0.003	1.6	0.2
HNC	0.1	10	10	CN (X $^2\Sigma^+$)	0.5	1	2.7	3.0×10^{-11} [e]	0.15	30	80
HCN	2.5E(5)	2.5E(4)	2000	CN (X $^2\Sigma^+$)	0.5	1	2.7	4.6×10^{-15} [f]	6	1	0.25
HCCN (^{3}A″)	0.25	2	0.2	HCCN (^{3}A″)	0.25	2	0.2	5.0×10^{-11} [d]	0.03	20	0.02
HNC	0.1	10	10	C_3N (X $^2\Sigma^+$)	1.5	0.4	0.005	3.0×10^{-11} [e]	0.5	12	0.15
HCN	2.5E(5)	2.5E(4)	2000	C_3N (X $^2\Sigma^+$)	1.5	0.4	0.005	3.0×10^{-11} [e]	1E(6)	3E(4)	30
HC_3N	5000	80	2.7	CN (X $^2\Sigma^+$)	0.5	1	2.7	1.7×10^{-11} [g]	4000	130	12

[a] Reactant concentrations in molecule cm^{-3}, at altitudes of 800, 1000, and 1200 km, were obtained by graphical interpolation of data presented in the modeling studies of Banaszkiewicz et al. (ref 29: HCN, HC_3N, N), Yung (ref 10: CN), and Toublanc et al. (ref 15: HCCN, C_3N), but with the [HCCN] value scaled downward by 2 orders of magnitude (see text; see also ref 17). The HNC estimate adopted here is the lowest of several cases modeled in a preliminary study (ref 19) of HNC formation in Titan's atmosphere. [b] Rate coefficients in cm^3 molecule^{-1} s^{-1}, at T = 200 K. [c] Calculated reaction rate for the specified process, at the indicated altitude. [d] Value recommended in ref 10 and adopted in the subsequent Titanian models (refs 15, 16, 29). [e] Refs 8, 9. [f] Ascribed rate coefficient for an exothermic radical/unsaturated neutral reaction lacking an activation barrier. [g] Ref 43.

Does the efficiency of reactions 5 and 6 as HNC loss processes also allow us to establish that these are, indeed, important sources of dicyanopolyynes? The Titanian atmospheric abundance of HNC has not yet been adequately modeled: a preliminary study has suggested a peak concentration, at altitude z = 1100 km, of [HNC] $\sim 10^4-10^5$ molecule cm^{-3}, although this must be treated as a raw estimate at best. This is also the approximate altitude of the triplet HCCN concentration peak, according to a recent model,[15] with [HCCN] $\sim 2.5 \times 10^5$ molecule cm^{-3}: i.e., up to 25 times greater than this HNC concentration estimate. However, existing models omit the crucial and apparently rapid reactions of HCCN (^{3}A″) with H (^{2}S) and with CH_3 (^{2}A′).[17] In the discussion that follows, we assume[17] that the published model HCCN (^{3}A″) concentration[15] is *at least* 2 orders of magnitude too high.

A crude indication of the relative importance of the various routes to NCCN (we reiterate that a detailed modeling study is necessary to reliably assess these matters) is given in Table 4, which compares estimated production rates at our three chosen altitude steps. The necessarily approximate values in this table suggest that the inefficient reaction of HCN with CN (reaction 1) dominates at low altitude, while the corresponding reaction of HNC (reaction 5) holds sway at 1000 km and above. This pattern reflects the expected production of HNC solely from high-altitude ion/electron recombination reactions,[19] while HCN is abundant at lower altitudes due to its production by various neutral/neutral processes. Note that while the kinetics of reaction 1 are reasonably well established (as is the Titanian atmospheric concentration of HCN), there is considerably more uncertainty regarding both the kinetics of reaction 5 and the true HNC concentration. Our assigned rate coefficient for this reaction is low in comparison to the 200 K values of $\sim 1-4 \times 10^{-10}$ cm^3 molecule^{-1} s^{-1} measured for several other reactions of unsaturated radicals with unsaturated neutrals.[44,45] Furthermore, with the scope that the HNC concentration could realistically[19] be an order of magnitude larger than the values ascribed here, there is a clear prospect that the true NCCN formation rate from Titanian HNC + CN may be much larger than the 1200 km peak value of 8×10^{-4} molecule cm^{-3} s^{-1} shown in Table 4. Reaction 5 clearly shows considerable promise as the probable dominant route to NCCN under the conditions applicable to Titan's outer atmosphere, a conclusion which may well apply also to other outer-planetary atmospheres.

What of NCCCCN production? Here there are four apparent production routes: reactions 4, 6, 7, and 8

$$C_3N + HCN \rightarrow NCCCCN + H \quad (7)$$

$$CN + HC_3N \rightarrow NCCCCN + H \quad (8)$$

with previous modeling studies featuring only reactions 4 and 8.[10,15,16] By analogy with the comparison of NCCN production rates, we have also assessed reactions 4, 6, 7, and 8 as NCCCCN sources, as detailed in Table 4. In this case, the reaction involving HNC (6) does not significantly impact on the apparent overall dicyanopolyyne production rate at any altitude, with the existing model reaction 8 always outweighing reaction 6 by at least an order of magnitude. However, our other 'new' reaction (7) is apparently extremely effective as a source of NCCCCN, by virtue of the comparatively high modeled abundances of the reactants involved. This process should be comparatively readily susceptible to experimental study, and such a laboratory investigation is urged so as to determine its true low-temperature rate coefficient.

Can the Huygens probe, scheduled to begin a detailed study of Titan in late 2004, provide in situ verification (or invalidation) of the proposed changes to Titan's dicyanopolyyne chemistry? One inference apparent from Table 4 is that NCCN arises mainly by ionosphere-driven production and reaction of HNC, while NCCCCN is largely formed through reaction of photochemically produced HCN. Hence, the smaller dicyanopolyyne is formed predominantly at 1000 km and above, while NCCCCN is produced in greater quantity at 800 km than at higher altitudes. This altitudinal variation in the concentrations of the two dicyanopolyynes should be readily detectable by Huygens, even if the reactive intermediate HNC (which cannot be mass-spectrometrically distinguished from the more abundant HCN) is not directly observable. Results from the Huygens probe will be keenly awaited, while laboratory study of the new reactions, and their inclusion in detailed kinetic models of Titan's upper atmosphere, would also be very welcome developments.

Conclusions

CCSD(T)/aug-cc-pVTZ/B3-LYP/6-311G** calculations confirm the results of an earlier CBS−RAD study showing that the reaction between CN (X $^2\Sigma^+$) and HNC leads most directly to products NCCN + H (^{2}S) without any barriers protruding above the total energy of reactants. In consequence, this process is now identified as the probable major route to the NCCN that has been detected within the upper atmosphere of the Saturnian satellite Titan. Our calculations on the C_4HN_2 surface, using the same level of theory for geometry optimizations and frequency calculations but the more economical CCSD(T)/aug-cc-pVDZ method for determination of single-point total energies, similarly show that the previously unstudied reaction of

C_3N ($X\ ^2\Sigma^+$) and HNC leads to a variety of possible products, with NCCCCN + H (^2S) likely dominant. While the C_3N + HNC reaction is also relevant to Titanian atmospheric chemistry, it is apparently outweighed as a source of NCCCCN by other processes occurring on the same surface, most notably reaction of C_3N ($X\ ^2\Sigma^+$) with HCN. Laboratory study of the latter process, which has not received any prior investigation, is urged so as to more properly assess its potential as a major reaction within Titan's atmosphere. Also highly recommended in this regard is the inclusion of the new reaction processes, explored here, within detailed kinetic models of Titan's upper atmosphere.

Acknowledgment. The authors thank the Australian Partnership for Advanced Computing, housed at the Australian National University Supercomputer Facility (S.P.), and the computer center of the Institute for Molecular Science, Japan (Y.O.) for generous access to computational resources. This research was partly supported by the Grants-in-Aid for Scientific Research on Priority Areas from the ministry of Education, Science, and Culture, Japan (Y.O.).

References and Notes

(1) Kunde, V. G.; Aikin, A. C.; Hanel, R. A.; Jennings, D. E.; Maguire, W. C.; Samuelson, R. E. *Nature* **1981**, *292*, 686.
(2) Coustenis, A.; Bezard, B.; Gautier, D.; Martin, A.; Samuelson, R. *Icarus* **1991**, *89*, 152.
(3) Perera-Jarmer, M. A.; Khanna, R. K.; Samuelson, R. E. *Bull. Am. Astron. Soc.* **1986**, *18*, 808.
(4) Samuelson, R. E.; Mayo, L. A.; Knuckles, M. A.; Khanna, R. K. *Planet. Space Sci.* **1997**, *45*, 941.
(5) Yung, Y. L.; Allen, M.; Pinto, J. P. *Astrophys. J. Suppl. Ser.* **1984**, *55*, 465.
(6) Li, X.; Sayah, N.; Jackson, W. M. *J. Chem. Phys.* **1984**, *81*, 833.
(7) Zabarnick, S.; Lin, M. C. *Chem. Phys.* **1989**, *134*, 185.
(8) Yang, D. L.; Yu, T.; Lin, M. C.; Melius, C. F. *J. Chem. Phys.* **1992**, *97*, 222.
(9) Wooldridge, S. T.; Hanson, R. K.; Bowman, C. T. *Int. J. Chem. Kinet.* **1996**, *28*, 245.
(10) Yung, Y. L. *Icarus* **1987**, *72*, 468.
(11) Fell, B.; Rivas, I. V.; McFadden, D. L. *J. Phys. Chem.* **1981**, *85*, 224.
(12) Takayanagi, T.; Kurosaki, Y.; Misawa, K.; Sugiura, M.; Kobayashi, Y.; Sato, K.; Tsunashima, S. *J. Phys. Chem. A* **1998**, *102*, 6251.
(13) Takayanagi, T.; Kurosaki, Y.; Yokoyama, K.; Sato, K.; Tsunashima, S. *Chem. Phys. Lett.* **1999**, *312*, 503.
(14) Balucani, N.; Alagia, M.; Cartechini, L.; Casavecchia, P.; Volpi, G. G.; Sato, K.; Takayanagi, T.; Kurosaki, Y. *J. Am. Chem. Soc.* **2000**, *122*, 4443.
(15) Toublanc, D.; Parisot, J. P.; Brillet, J.; Gautier, D.; Raulin, F.; McKay, C. P. *Icarus* **1995**, *113*, 2.
(16) Lara, L. M.; Lellouch, F.; Lopez-Moreno, J. J.; Rodrigo, R. *J. Geophys. Res. E* **1996**, *101*, 23261.
(17) Osamura, Y.; Petrie, S. *J. Phys. Chem. A* **2004**, *108*, 3615.
(18) Petrie, S.; Millar, T. J.; Markwick, A. J. *Mon. Not. R. Astron. Soc.* **2003**, *341*, 609.
(19) Petrie, S. *Icarus* **2001**, *151*, 196.
(20) Herbst, E. *Astrophys. J.* **1978**, *222*, 508.
(21) Talbi, D.; Ellinger, Y. *Chem. Phys. Lett.* **1998**, *288*, 155.
(22) Shiba, Y.; Hirano, T.; Nagashima, U.; Ishii, K. *J. Chem. Phys.* **1998**, *108*, 698.
(23) Jursic, B. S. *J. Mol. Struct. (THEOCHEM)* **1999**, *487*, 211.
(24) Tachikawa, H. *Phys. Chem. Chem. Phys.* **1999**, *1*, 4925.
(25) Ip, W. H. *Astrophys. J.* **1990**, *362*, 354.
(26) Keller, C. N.; Cravens, T. E.; Gan, L. *J. Geophys. Res. A* **1992**, *97*, 12117.
(27) Keller, C. N.; Anicich, V. G.; Cravens, T. E. *Planet. Space Sci.* **1998**, *46*, 1157.
(28) Galand, M.; Lilensten, J.; Toublanc, D.; Maurice, S. *Icarus* **1999**, *140*, 92.
(29) Banaszkiewicz, M.; Lara, L. M.; Rodrigo, R.; Lopez-Moreno, J. J.; Molina-Cuberos, G. J. *Icarus* **2000**, *147*, 386.
(30) Mayer, P. M.; Parkinson, C. J.; Smith, D. M.; Radom, L. *J. Chem. Phys.* **1998**, *108*, 604.
(31) Petrie, S. *J. Phys. Chem. A* **2002**, *106*, 11181.
(32) Becke, A. D. *J. Chem. Phys.* **1993**, *98*, 5648.
(33) Lee, C.; Yang, W.; Parr, R. G. *Phys. Rev. B* **1988**, *37*, 785.
(34) Krishnan, R.; Binkley, J. S.; Seeger, R.; Pople, J. A. *J. Chem. Phys.* **1980**, *72*, 650.
(35) Frisch, M. J.; Trucks, G. W.; Schegel, H. B.; Scuseria, G. E.; Robb, M. A.; Cheeseman, J. R.; Zakrzewski, V. G.; Montgomery, J. A., Jr.; Stratmann, R. E.; Burant, J. C.; Dapprich, S.; Millam, J. M.; Daniels, A. D.; Kudin, K. N.; Strain, M. C.; Farkas, O.; Tomasi, J.; Barone, V.; Cossi, M.; Cammi, R.; Mennucci, B.; Pomelli, C.; Adamo, C.; Clifford, S.; Ochterski, J. W.; Petersson, G. A.; Ayala, P. Y.; Cui, Q.; Morokuma, K.; Malick, D. K.; Rabuck, A. D.; Raghavachari, K.; Foresman, J. B.; Cioslowski, J.; Ortiz, J. V.; Stefanov, B. B.; Liu, G.; Liashenko, A.; Piskorz, P.; Komaromi, I.; Gomperts, R.; Martin, R. L.; Fox, D. J.; Keith, T.; Al-Laham, M. A.; Peng, C. Y.; Nanayakkara, A.; Gonzalez, C.; Challacombe, M.; Gill, P. M. W.; Johnson, B. G.; Chen, W.; Wong, M. W.; Andres, J. L.; Head-Gordon, M.; Replogle, E. S.; Pople, J. A. GAUSSIAN98; Gaussian, Inc.: Pittsburgh, PA, 1998.
(36) Amos, R. D.; Bernhardsson, A.; Berning, A.; Celani, P.; Cooper, D. L.; Deegan, M. J. O.; Dobbyn, A. J.; Eckert, F.; Hampel, C.; Hetzer, G.; Knowles, P. J.; Korona, T.; Lindh, R.; Lloyd, A. W.; McNicholas, S. J.; Manby, F. R.; Meyer, W.; Mura, M. E.; Nicklass, A.; Palmieri, P.; Pitzer, R.; Rauhut, G.; Schutz, M.; Schumann, U.; Stoll, H.; Stone, A. J.; Tarroni, R.; Thorsteinsson, T.; Werner, H. J. MOLPRO 2002: Birmingham, U. K., 2002.
(37) Kendall, R. A.; Dunning, T. H.; Harrison, R. J. *J. Chem. Phys.* **1992**, *96*, 6796.
(38) Balucani, N.; Asvany, O.; Chang, A. H. H.; Lin, S. H.; Lee, Y. T.; Kaiser, R. I.; Osamura, Y. *J. Chem. Phys.* **2000**, *113*, 8643.
(39) Stahl, F.; Schleyer, P. v. R.; Bettinger, H. F.; Kaiser, R. I.; Lee, Y. T.; Schaefer, H. F., III *J. Chem. Phys.* **2001**, *114*, 3476.
(40) Kaiser, R. I.; Vereecken, L.; Peeters, J.; Bettinger, H. F.; Schleyer, P. v. R.; Schaefer, H. F., III *Astron. Astrophys.* **2003**, *406*, 385.
(41) In general, structures optimized at the B3-LYP/6-311G** level of theory correspond closely to the QCISD/6-31G* geometries. The latter geometries have been detailed previously in ref 18 and thus are not shown in the present work.
(42) Fukuzawa, K.; Osamura, Y. *Astrophys. J.* **1997**, *489*, 113.
(43) Halpern, J. B.; Miller, G. E.; Okabe, H. *Chem. Phys. Lett.* **1989**, *155*, 347.
(44) Sims, I. R.; Queffelec, J.-L.; Travers, D.; Rowe, B. R.; Herbert, L. B.; Karthauser, J.; Smith, I. W. M. *Chem. Phys. Lett.* **1993**, *211*, 461.
(45) Carty, D.; Le Page, V.; Sims, I. R.; Smith, I. W. M. *Chem. Phys. Lett.* **2001**, *344*, 310.